Relaxation times of $BP_{1-x}BPI_x$ mixed crystals: Atypical dipolar glass behavior of the average local potential asymmetry

J. Banys,* J. Macutkevic, and S. Lapinskas
Faculty of Physics, Vilnius University, Saulėtekio 9, LT-10222 Vilnius, Lithuania

C. Klimm and G. Völkel
Fakultät für Physik und Geowissenschaften, Universität Leipzig, D-04103 Leipzig, Germany

A. Klöpperpieper
Fakultät für Physik, Universität des Saarlandes, D-66123 Saarbrücken, Germany
(Received 24 October 2005; revised manuscript received 15 February 2006; published 14 April 2006)

Dielectric susceptibility measurements in a wide frequency spectrum were used to obtain the distribution of the relaxation times of $BP_{1-x}BPI_x$ mixed crystals. The dipole freezing results in a broad distribution of the relaxation times. The parameters of the double-well potentials of the hydrogen bonds, the local polarization distribution function and glass order parameter have been extracted from the dielectric measurements. The microscopic parameters are in good agreement with magnetic resonance data. The average local potential asymmetry A_0 shows a behavior different from that of RADP. Dielectric spectroscopy gives the new and surprising result that the nonzero mean J_0/k_B of the random bond interaction is vanishing for very low temperatures. One can suspect that it is related to the transition into the low-temperature nonergodic glassy phase.

DOI: 10.1103/PhysRevB.73.144202 PACS number(s): 77.22.Gm, 02.30.Rz, 64.70.Pf, 77.84.Fa

I. INTRODUCTION

The two almost isostructural compounds betaine phosphite (BPI) $(CH_3)_3NCH_2COOH_3PO_3$, and betaine phosphate (BP) $(CH_3)_3NCH_2COOH_3PO_3$ form solid solutions at any concentration.[1–4] Similar to the KDP family, mixed crystals $BP_{1-x}BPI_x$ of antiferroelectric betaine phosphate and ferroelectric betaine phosphite show an interesting phase diagram with phase transitions to long-range ordered ferroelastic, ferroelectric, and antiferroelectric phases or to glassy states in dependence on the ratio x of the two compounds.[5–9] The structure of both compounds[10,11] is very similar. The inorganic tetrahedral PO_4 or HPO_3 groups are linked by hydrogen bonds forming zig-zag chains along the monoclinic b axis. The betaine molecules are arranged almost perpendicular to these chains along the a direction and linked by one (BPI) or two (BP) hydrogen bonds to the inorganic group.

Both compounds, BPI and BP, undergo a phase transition from a paraelectric high-temperature phase with space group $P2_1/m$ to an antiferrodistortive phase with space group $P2_1/c$ at 355 K (BPI) and 365 K (BP), respectively. In the high-temperature phase the PO_4 or HPO_3 groups and the betaine molecules are disordered. They both order in the antiferrodistortive phase, but the hydrogen atoms linking PO_4 or HPO_3 groups remain disordered. Ordering of these hydrogen atoms induces the phase transition into the ferroelectric or antiferroelectric phase. BPI experiences a transition into a ferroelectric ordered low-temperature phase with space group $P2_1$ at 220 K. BP shows two further structural transitions at 86 K into a ferroelectric intermediate phase of $P2_1$ symmetry[12] and at 81 K into an antiferroelectric low-temperature phase with doubling of the unit cell along the crystallographic a direction.

The temperature dependence of the dielectric permittivity of both compounds shows evidence for a quasi-one-dimensional behavior. The coupling between the electric dipolar units within the chains is much stronger than that one between dipolar units in neighboring chains.[11,13] Antiferroelectric order is established in BP at $T_C=81$ K (Ref. 1) in such a way that the O-H···O bonds order ferroelectrically within the one-dimensional chains, whereas neighboring chains are linked antiferroelectrically.[10] In BPI, however, neighboring chains are linked ferroelectrically below $T_C=216$ K.[3]

Deuteration of hydrogen-bonded ferroelectrics leads to significant changes of the dielectric properties and shifts the phase transition temperature to higher values.[10] This isotope effect has already been studied in deuterated crystals of the betaine family, namely betaine phosphate (DBP) and betaine phosphite (DBPI).[1,14] The low-frequency dielectric measurements of DBPI showed[14] that the transition temperature is shifted up to 297 K. Deuterated BP (DBP) shows only two transitions, one at 365 K into the ferrodistortive phase and another one at 119 K into the antiferroelectric phase. The ferroelectric phase that exists in normal BP is missing in deuterated BP. This gives strong evidence that the hydrogen bonds play an important role in the ferroelectric and antiferroelectric transition.

In the mixed crystals the competing ferroelectric and antiferroelectric interactions cause a glasslike order behavior of the protons in the system of hydrogen bonds.[5–9] Such materials belong to a class of orientational glasses that are called proton glasses.[15] The proton glasses are of special interest in so far as they can contribute to the basic understanding of the glassy behavior of matter as model systems. Theoretical descriptions have been developed for them, which allow comparisons with the experimental results.[16–19]

The phase diagram of $BP_{1-x}BPI_x$ (Refs. 7, 9, and 20) which was known until now can be characterized by three regions: a first one with concentration $x<0.3$ where a transition into an antiferroelectric ordered state appears, a second one with $0.9>x>0.3$ in which glassy behavior is observed at low temperatures, and a third region with a ferroelectric ordered low temperature phase for $x>0.9$. Dielectric measurements[5,8,9,20,21] revealed proton glass behavior for $x=0.85$, 0.80, 0.60, 0.50, and 0.40.

Very recently, a systematic study of the dielectric properties of compounds of the series $BP_{1-x}BPI_x$ was presented[20] in the paraelectric phase, and compared with the predictions of three microscopic models: the quasi-one-dimensional Ising model without disorder,[22–24] the Sherrington-Kirkpatrick model,[25] and the quasi-one-dimensional random-bond random-field Ising model.[19] From the analysis of the temperature dependent static susceptibility, parameters were determined characterizing the dipolar interactions and the random electric fields in these systems. Only in one of the compounds with the lowest admixture of betaine phosphite, $x_{sol}=0.15$, a behavior consistent with a quasi-one-dimensional glass phase was found.[20] There was no evidence of quasi-one-dimensional behavior for compounds with a higher concentration of BPI except for nearly pure ferroelectric BPI. In fact, the other compounds with a glass phase were rather well fitted by the three-dimensional RBRF Ising model with the inclusion of random fields.

In these compounds, the random fields are of greater importance than the random bonds. It was suspected that substitutional disorder leads to a more isotropic dielectric behavior where interchain and intrachain couplings are similar in magnitude. The Almeida-Thouless temperatures were estimated for all the compounds with a glass phase and found to be close to the temperature where the real part of the low frequency dielectric constant has its maximum.

Nuclear magnetic resonance (NMR) proved to be one of the most appropriate techniques for the study of local proton or deuteron order and dynamics.[16–18] Deuteron glasses were carefully analyzed by D^2 NMR where the local deuteron order is monitored by the nuclear quadrupole coupling. However, there is no direct study of the proton order in a proton glass by H^1 NMR up to now because it is difficult to resolve local proton order from the chemical shift data.

Recently we reported on direct studies of the local proton order by means of high resolution electron spin resonance (ESR) measurements such as CW and pulsed electron nuclear double resonance (ENDOR), electron spin echo (ESE), and electron spin echo envelope modulation (ESEEM) (Refs. 26–28) on the PO_3^{2-} paramagnetic probe in the x-irradiated proton glasses $BP_{0.15}BPI_{0.85}$ and $BP_{0.40}BPI_{0.60}$. Hydrogen bonds link the phosphite and phosphate groups to quasi-one-dimensional chains along the crystallographic *b* direction. We showed that the protons in these bonds order glasslike. The ENDOR line shape of this proton manifold is a direct mirror of the local order parameter distribution function $w(p)$ of the protons in the hydrogen bonds. This allows a very detailed comparison with theoretical models such as the one- and three-dimensional random-bond random-field (RBRF) Ising glass model because for one given temperature one has not only one single measuring point as for the static susceptibility but an entire order parameter distribution curve.

The experimental Edwards-Anderson glass order parameter was obtained as the second moment of $w(p)$. From its temperature dependence the variance of the random bond interaction and the variance of the random local fields were calculated. For both compounds, the results are characteristic for a proton glass with strong random fields. The unusually strong random fields reflect the relatively strong distortions of the proton double well potentials in the hydrogen bonds adjacent to substituted phosphate sites.

We have to mention that the stable inorganic PO_3^{2-} radical studied in several solid solutions $BP_{1-x}BPI_x$ with ESR techniques is created only at the HPO_3 but not at the PO_4 fragments. Consequently, we also can probe the mixed crystals at the HPO_3 sites only. On the other hand, beyond all doubt, we may presuppose from our experiences with pure betaine phosphite that measurements of the PO_3^{2-} probe give representative evidence of the proton configuration at HPO_3 sites without noticeable distortions due to the radical formation. Therefore, in the phosphite-rich compositions of $BP_{1-x}BPI_x$ where the phosphate units may be understood as substitutional defects, the measured proton configurations at the PO_3^{2-} probe are more or less representative for the general proton behavior.

In the phosphate-rich $BP_{1-x}BPI_x$ compositions, however, the statistically incorporated HPO_3 fragments have to be considered as substitutional defects, which create internal stochastic electric fields. From ENDOR studies of the PO_3^{2-} paramagnetic probe on the phosphate-rich side of the $BP_{1-x}BPI_x$ solid solution we got experimental evidence that the protons in the hydrogen bonds of a PO_4-HPO_3-PO_4 segment see an asymmetric double well potential which is a demonstration of the polar defect character of this segment. The polarity of the defect segment along the *b*-direction depends on which side, left or right, of the zig-zag chain the HPO_3 defect is incorporated. It is of importance that the polarity can change under the influence of an ordering field. The same conclusion may be drawn for a PO_4 defect in a HPO_3 chain.

For $BP_{0.15}BPI_{0.85}$ and $BP_{0.40}BPI_{0.60}$ it must be mentioned that the correspondence of the experimental order parameter distribution function with the simulations could be improved considerably if a nonzero mean $J_0/k_B=200$ K and 212 K of the random bond interaction and a tunneling energy were considered in the three-dimensional RBRF Ising model. Additionally, in order to obtain a better agreement with the experimental $w(p)$ behavior, the variance of the random fields had to be reduced from a constant value at temperatures above J_0/k_B to temperature dependent lower values below J_0/k_B. This reduction of the random field magnitude is caused by the reorientation of the polar defect units under the influence of an ordering field as mentioned above. The results indicate a smeared transition at $T_0=144$ K and 160 K for $BP_{0.15}BPI_{0.85}$ and $BP_{0.40}BPI_{0.60}$, respectively, into a phase with a mean long-range order in the proton chains but with strong fluctuations of the local order parameters. This additional phase transition is also reflected in a temperature anomaly of the electron spin-lattice relaxation indicating a singular anomaly in the phonon system.[29–31] It was shown

that the infrared active optical mode at 560 cm^{-1} experiences a critical damping by interacting with a critical soft mode related to the mentioned transition. These ENDOR and electron spin-lattice relaxation results were recently confirmed by infrared measurements.[32] Both the measurements show that the transition is not of local but of collective nature.

Though there are indications of a proton glass behavior, the local measurements showed that the system is more complex. One comes to the conclusion that for the solid solutions $BP_{1-x}BPI_x$, with compositions $x=0.05, 0.15, 0.30, 0.60, 0.85, 0.94$, a phase with glassy order exists above a certain temperature T_0. Below this temperature T_0 an inhomogeneous ferric phase appears with coexisting long-range and glassy proton order like in $Rb_{1-x}(NH_4)_xH_2AsO_4$.[18]

Very recently we published dielectric susceptibility measurements of $BP_{0.15}BPI_{0.85}$ in a wide frequency spectrum and presented the data analysis.[33] Solving the integral equation for the susceptibility with the Tikhonov regularization technique, this method allows the extraction of the distribution of the relaxation times and resolves multiple dynamical processes. The dielectric relaxation spectrum is described in terms of an ensemble of Debye processes with a continuous relaxation time distribution $w(\tau)$. Unfortunately, the direct extraction of $w(\tau)$ from $\varepsilon^*(\nu)$ is a mathematically ill-posed problem. This difficulty may be one of the reasons why the spectra are usually treated as superposition of a few parameterized functions. If a direct calculation of $w(\tau)$ from $\varepsilon^*(\nu)$ can be reliably performed, in a manner similar to the Fourier transformation between time and frequency domains, then several problems arising from the use of empirical functions can be avoided. Having obtained $w(\tau)$ one can then seek a physical interpretation in the τ domain rather than in the frequency domain.

The dipole-freezing phenomena result in a broad asymmetrical distribution of the relaxation times. We demonstrated that the parameters of the double-well potentials of the hydrogen bonds, the local polarization distribution function and the glass order parameter can be extracted from the dielectric measurements. The microscopic parameters obtained are in good agreement with magnetic resonance data.

With the present paper we extend these wide band dielectric susceptibility measurements and this data analysis on a series of protonated ($x=0.50, 0.60, 0.70$) and deuterated ($x=0.50, 0.60, 0.70, 0.75, 0.85$) solid solutions of $(BP)_{1-x}(BPI)_x$. It will be demonstrated that besides magnetic resonance techniques the dielectric spectroscopy coupled with the data analysis presented above is another appropriate tool to determine microscopic glass parameters. Because peculiarities do not exist with the magnetic resonance line shape in the slow motion limit, dielectric spectroscopy gives interesting results, especially for low temperatures. The measurements give further indications of an intermediate inhomogeneous long-range ordered phase for a wider range of compositions as already concluded from ENDOR and electron spin-lattice time measurements.[26–31] Over and above that, dielectric spectroscopy gives the surprising result that the nonzero mean J_0/k_B of the random bond interaction is vanishing for very low temperatures. One can suspect that it is related to the transition into the low-temperature nonergodic glassy phase.

II. EXPERIMENT

$BP_{1-x}BPI_x$ and $DBP_{1-x}DBPI_x$ mixed crystals with $x=0.50, 0.60, 0.70$ and $x=0.50, 0.60, 0.70, 0.75$, respectively, were grown by controlled evaporation from H_2O and D_2O solutions containing betaine with 100× percentage of H_3PO_4 and the rest of H_3PO_3. By analogy with DBPI (Ref. 14) one expects that only the protons in the O-H···O bonds of the inorganic H_3PO_4 and H_3PO_3 should be replaced by deuterons. For the dielectric spectroscopy, gold plated single crystals were oriented along the monoclinic b axis. The complex dielectric constant $\varepsilon^*=\varepsilon'-i\varepsilon''$ was measured by a capacitance bridge HP4284A in the frequency range 20 Hz to 1 MHz. The typical sample size was 50 mm^2 area and 0.7 mm thickness. The value of the measurement voltage was 0.5 V. Further decrease of the measurement voltage does not change the results for the dielectric permittivity. All measurements have been performed on heating with the rate of about 0.5 K/min in the dielectric dispersion region. No differences in the value of the dielectric permittivity have been observed for cooling and heating due to the low value of the measurement field and the absence of temperature gradients in the sample. The temperature was measured with a calibrated silicon diode (Lake Shore type DT-470-DI-13). For the temperature-dependent measurements a Leybold VSK-4-320 cryostat was used.

III. RESULTS

For all mixed crystals under study no anomaly in ε' indicating a polar phase transition can be detected down to the lowest temperatures. In the temperature region below 100 K dispersion effects dominate the dielectric response in the frequency range under study (Fig. 1). The temperature behavior of ε' and ε'' seems to be typical for glasses: with decreasing measurement frequency the maximum of ε' shifts to lower temperatures followed by the maximum of ε''. At fixed temperatures the frequency dependence of ε' and ε'' provides clear evidence that the frequency dependence of ε'' is much broader than for Debye dispersion (Fig. 2), thus there is a distribution of the relaxation times. As it is possible to see from experiment, the distribution of the relaxation times becomes broad, especially at low temperatures over three decades. Each one of the traditional models is strictly fixed with respect to the shape of the relaxation-time distribution function. The Cole-Cole formula assumes a symmetrically shaped distribution of the relaxation times, but the real distribution function can be different from this.

In order to get information that is more precise about the real relaxation-time distribution function, a special approach has been developed. We assume that the real and imaginary parts of the dielectric spectrum can be represented as a superposition of independent individual Debye-type relaxation processes[34–36]

$$\varepsilon' = \varepsilon_\infty + \int_{-\infty}^{\infty} \frac{w(\tau) d \ln \tau}{1 + (2\pi\nu\tau)^2}, \tag{1a}$$

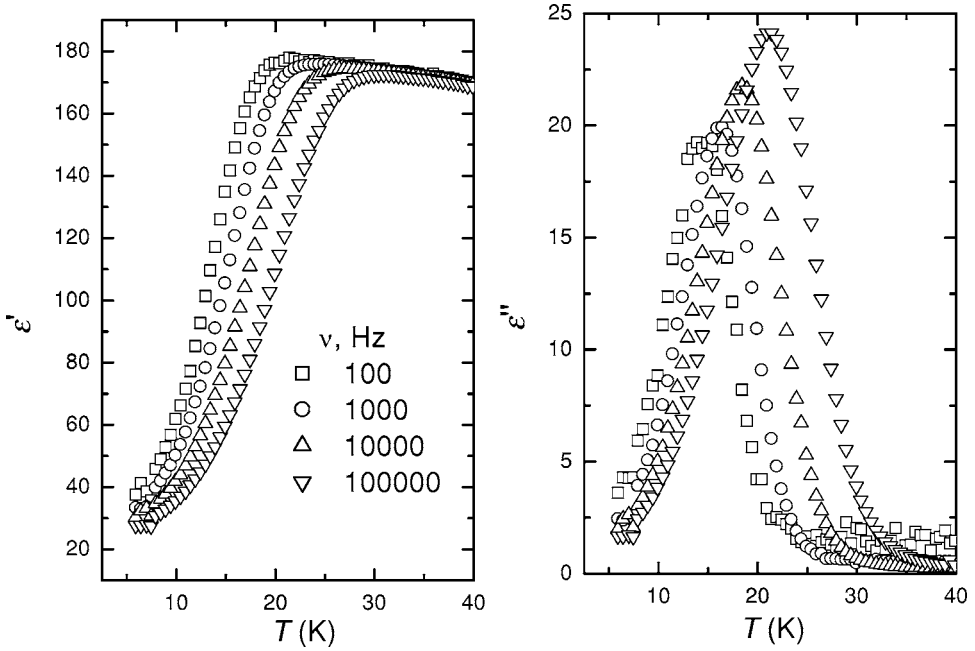

FIG. 1. The temperature dependence of complex dielectric permittivity of $BP_{0.3}BPI_{0.7}$ crystals.

$$\varepsilon'' = \int_{-\infty}^{\infty} \frac{(2\pi\nu\tau)w(\tau)d\ln\tau}{1+(2\pi\nu\tau)^2}. \tag{1b}$$

Actually, these two expressions are the first kind Fredholm integral equations for the definition of the relaxation-time distribution function $w(\tau)$. Such integral equations are known to be an ill-posed problem. The most general method of considering them is the Tikhonov regularization.[37] Numerical treatment of the integral equations (1) requires a discretization, which leads to a set of linear nonhomogeneous algebraic equations. In the matrix notation it can be represented as

$$\mathbf{AX} = \mathbf{T}. \tag{2}$$

Here the components T_n $(1<n<N)$ of the vector **T** represent the dielectric spectrum $(\varepsilon_i', \varepsilon_i'')$, $(1<i<N/2)$ recorded at some frequency intervals n_i. We used equidistant frequency intervals in the logarithmic scale $\Delta \ln \nu_m = \text{const}$. The components X_m $(1<m<M)$ of the vector **X** stand for the relaxation time distribution $w(\tau)$ that we are looking for. The symbol **A** stands for the kernel of the above matrix equation. It represents the matrix with elements obtained by the direct substitution of n_i and τ values into the kernels of the integral equations (1).

Usually the number of data points N exceeds the number of spectrum points M. Due to the fact that Eq. (2) cannot be

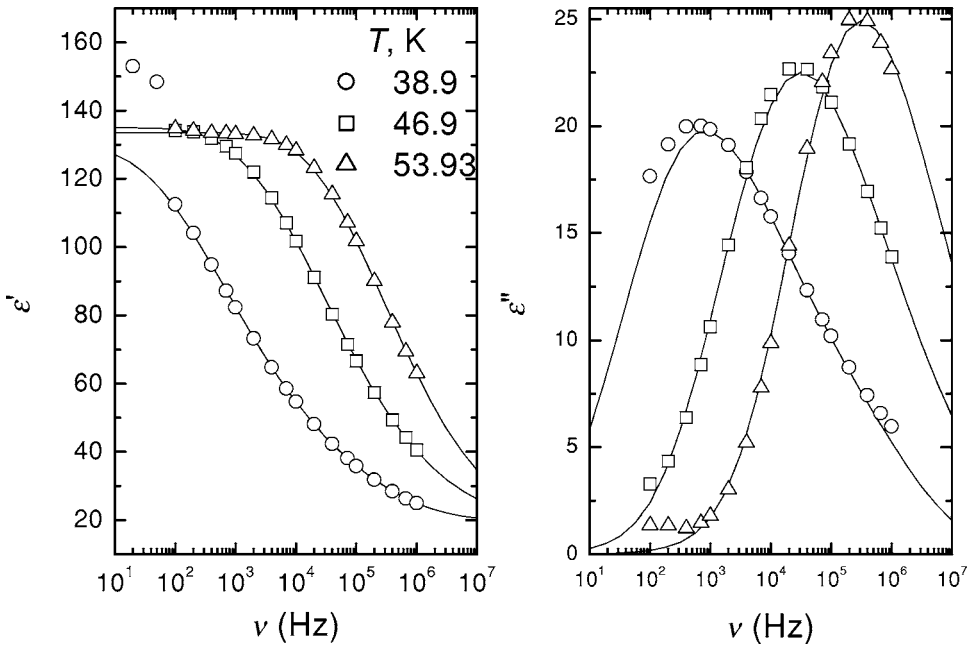

FIG. 2. The frequency dependence of complex dielectric permittivity of $DBP_{0.3}DBPI_{0.7}$ crystals.

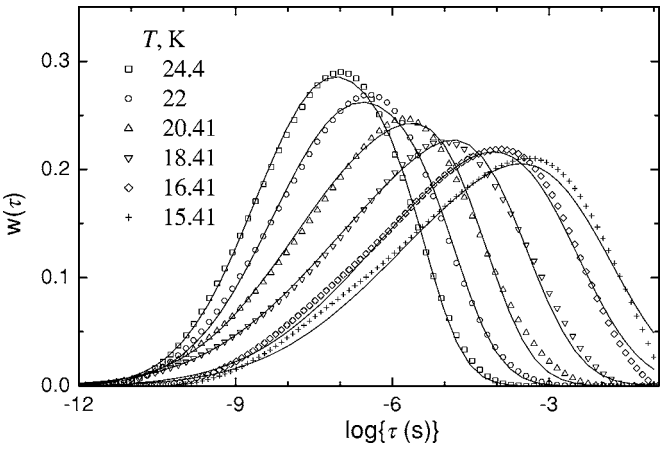

FIG. 3. The distributions of relaxation times of $BP_{0.3}BPI_{0.7}$ crystals.

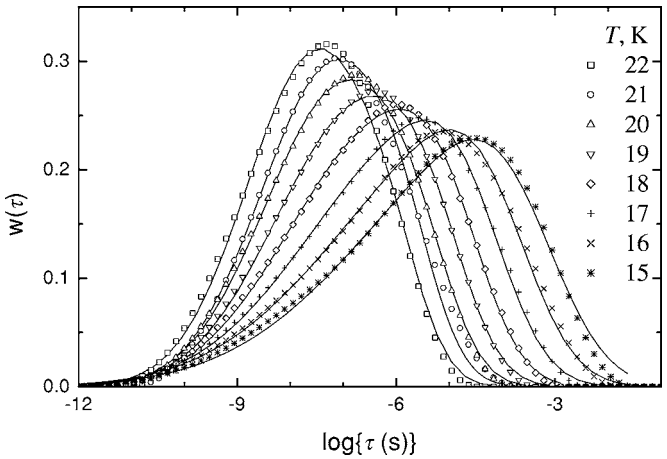

FIG. 4. The distributions of relaxation times of $BP_{0.4}BPI_{0.6}$ crystals.

solved directly, it is replaced by the minimization of the following function:

$$\Phi_0 = \|\mathbf{T} - \mathbf{AX}\|^2 = \min. \tag{3}$$

Here and further we shall use the following vector norm notation $\|V\|^2 = \|V^T\|\|V\|$, where the superscript T indicates the transposed vector or matrix. Due to the ill-posed nature of the integral Fredholm equations, the above minimization problem is ill-posed as well, and consequently, cannot be treated without some additional means. Thus, following the Tikhonov regularization procedure the functional Φ_0 is replaced by the expression

$$\Phi(\alpha) = \|\mathbf{T} - \mathbf{AX}\| + \alpha^2\|\mathbf{PX}\|^2 = \min \tag{4}$$

modified by an additional regularization term. The symbol **P** stands for the regularization matrix. The regularization parameter α plays the same role as a filter bandwidth when smoothing noisy data.

Usually there are many solutions satisfying Eq. (4) within the limit given by the experimentally recorded dielectric spectrum errors. Thus, it is necessary to take into consideration as many additional conditions as possible. First, we know that all relaxation-time distribution components have to be positive ($X_n > 0$). Next, sometimes one knows that rather reliable values of the static permittivity $\varepsilon(0)$ or of the limit high-frequency dielectric permittivity ε_∞. In this case, it is worthwhile to restrict the above minimization problem by fixing either of those values or both.

Usually the minimization problem of Eq. (4) is solved numerically by means of the least squares problem technique.[38] Following the algorithm described by Provencher[39] a program was developed which provides numerical solutions of the restricted minimization problem of Eq. (4) and extracts the relaxation-time distribution $w(\tau)$ (for details, see Ref. 33). The regularization parameter α is crucial for the shape of the distribution function of the relaxation times. Very small values of α result in artificial physically meaningless structures in $w(\tau)$, while very large α tends to oversmooth the shape of $w(\tau)$ and suppress information. Therefore, serious calculations have been performed starting from small to bigger values of α. With increasing values of α, the deviation between experimental and calculated spectra changes slowly initially, and then at a certain point starts to decrease rapidly. We considered this particular value of $\alpha = 4$ as the best one for our experiment.[34,39]

The relaxation time distributions of the mixed crystals under study calculated from the experimental dielectric spectra at different temperatures are presented in Figs. 3–9 as points. One can recognize the relaxation-time distribution does significantly broaden to lower temperatures. At low temperatures the relaxation-time distribution is spread out in a very wide region, as it is typical for dipolar glasses.

IV. COMPARISON OF THE RESULTS WITH THE DIPOLAR GLASS MODEL

For dipolar glasses, it is usually assumed that the proton motion in the double well O-H···O potentials is randomly frozen out at low temperatures, implying a static quenched disorder.[40] But due to the "built-in" disorder, always present

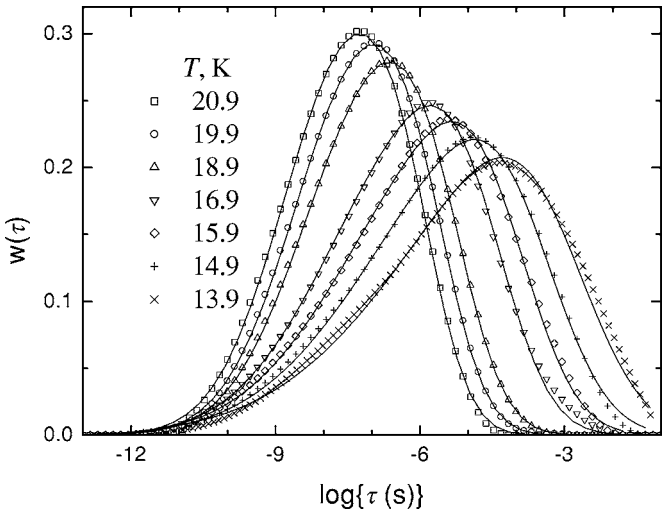

FIG. 5. The distributions of relaxation times of $BP_{0.5}BPI_{0.5}$ crystals.

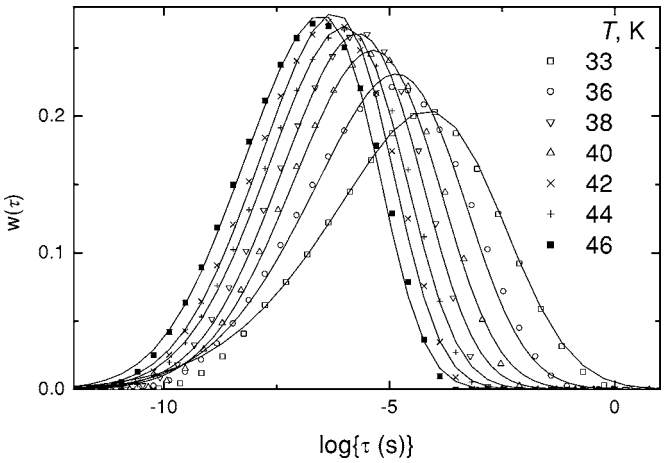

FIG. 6. The distributions of relaxation times of $DBP_{0.25}DBPI_{0.75}$ crystals.

in the off-stoichiometric solid solutions, there are a variety of environments for the O-H···O bonds. This leads to a distribution of the microscopic parameters of the bonds and, consequently, a distribution of dynamic properties such as the dipolar relaxation times when quenching takes place. A microscopic approach to dynamics based on correlated motion of Takagi groups through a Slater lattice has been published recently for RADP-type proton and deuteron glasses.[41] Here we will restrict the considerations to the usual mean-field approach.

We consider a proton or deuteron moving in an asymmetric double well potential. The movement consists of fast oscillations in one of the minima with occasional thermally activated jumps between the minima. Here we neglect quantum tunneling, which is negligible for deuterons although it might be significant for protons at low temperatures.

The jump probability is governed by the Boltzmann probability of overcoming the potential barrier between the minima. An ensemble of similar O-H···O bonds has a relaxational dielectric response at lower frequencies. It was shown that the relaxation time of an individual hydrogen bond dipole in such a system[42] is given by

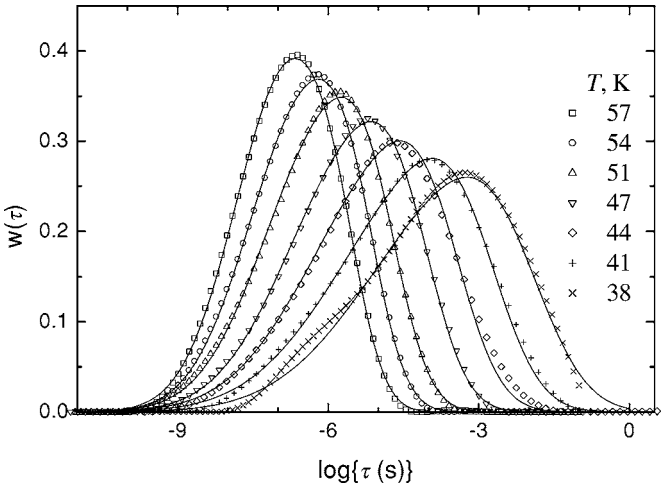

FIG. 7. The distributions of relaxation times of $DBP_{0.3}DBPI_{0.7}$ crystals.

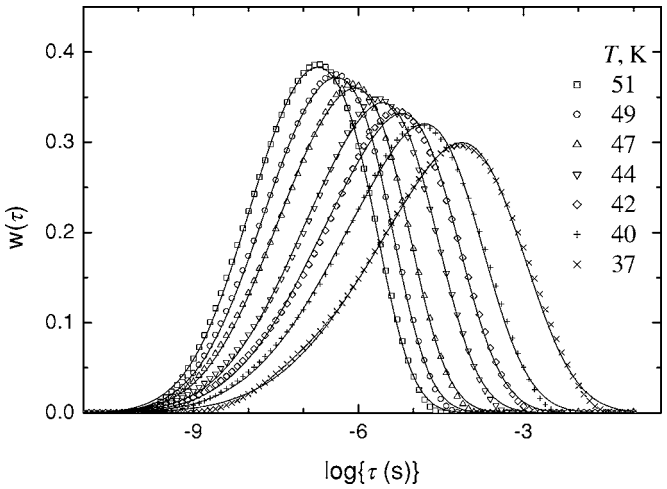

FIG. 8. The distributions of relaxation times of $DBP_{0.4}DBPI_{0.6}$ crystals.

$$\tau = \tau_0 \frac{\exp\left[\dfrac{E_b}{k_B(T-T_0)}\right]}{2\cosh\left[\dfrac{A}{2k_BT}\right]} \tag{5}$$

with $\tau_0 = 1/(2\pi\nu_\infty)$ where ν_∞ is the attempt frequency and T_0 is the Vogel-Fulcher temperature. The parameter A accounts for the asymmetry of the local potential produced by the mean-field influence of all the other dipoles. Thus, the local polarization

$$p = \tanh\left[\frac{A}{2k_BT}\right] \tag{6}$$

as the time-averaged dipole moment of an individual O-H···O bond is given by the asymmetry parameter A.[42] We are assuming that the parameter E_b does not change with temperature. Additionally, we are introducing the Vogel-Fulcher temperature T_0 that does effectively account for the increase of the barrier on approaching this temperature. We

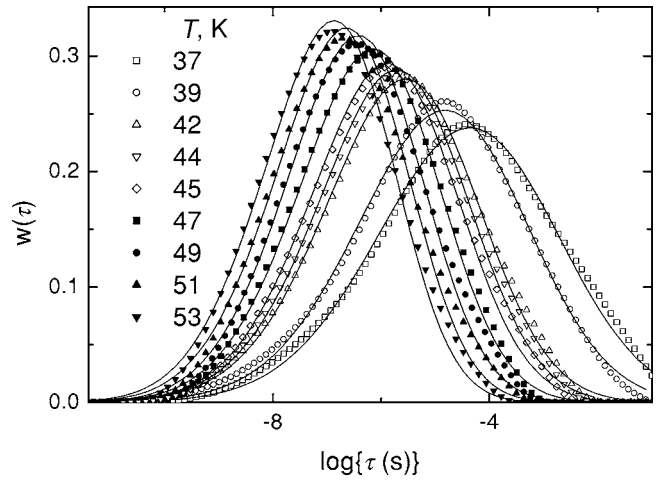

FIG. 9. The distribution of relaxation times of $DBP_{0.5}DBPI_{0.5}$ crystals.

further consider that the asymmetry A and the potential barrier E_b of the local potential of the O-H···O bonds both are randomly distributed around their mean values A_0 and E_{b0} according to a Gaussian law resulting in the distribution functions

$$w(E_b) = \frac{1}{\sqrt{2\pi}\sigma_{Eb}} \exp\left[\frac{(E_b - E_{b0})^2}{2\sigma_{Eb}^2}\right] \tag{7}$$

and

$$w(A) = \frac{1}{\sqrt{2\pi}\sigma_A} \exp\left[\frac{(A - A_0)^2}{2\sigma_A^2}\right], \tag{8}$$

where σ_{E_b} and σ_A are the standard deviations of E_b and A, respectively, from their mean values. The distribution function of relaxation times is then given by

$$w(\ln \tau) = \int_{-\infty}^{\infty} w(A) w(E_b(A,\tau)) \frac{\partial E_b}{\partial(\ln \tau)} dA, \tag{9}$$

where $E_b(A,\tau)$ is the dependence of E_b on A for a given τ, derived from Eq. (5). From the distribution function $w(A)$ of the local potential asymmetry the distribution function $w(p)$ of the local polarizations of the hydrogen bonds can easily be deduced

$$w(p) = \frac{2k_BT}{\sqrt{2\pi}\sigma_A(1-p^2)} \exp\left[-\frac{(a\tanh[p] - a\tanh[\bar{p}])^2}{2\sigma_A(2k_BT)^2}\right]. \tag{10}$$

This expression transforms into the form known for the random-bond random field (RBRF) model[17,18] when one substitutes

$$\sigma_A = 2J\sqrt{q_{\mathrm{EA}} + \tilde{\Delta}} \tag{11}$$

and

$$A_0 = 2J_0\bar{p}. \tag{12}$$

Here, J is the Gaussian variance and J_0 is the average of the random interbond coupling, $\tilde{\Delta} = \Delta/J^2$ is the renormalized variance of the random local electric fields, $\bar{p}$ is the average polarization, and q_{EA} the Edwards-Anderson glass order parameter. The latter two are defined as

$$\bar{p} = \int_{-1}^{+1} p w(p) dp \tag{13}$$

and

$$q_{\mathrm{EA}} = \int_{-1}^{+1} p^2 w(p) dp. \tag{14}$$

Fits with the experimentally obtained relaxation-time distributions shown in Figs. 3–9 were performed simultaneously for all the considered temperatures. For one given crystal, only one parameter set τ_0, T_0, E_{b0}/k_B, and σ_{E_b} shown in Table I was used for all the temperatures, whereas A and σ_A appeared to be temperature dependent. The fit results are presented in Figs. 3–9 as solid lines.

TABLE I. Parameters τ_0, T_0, E_{b0}/k_B, σ_{E_b}/k_B, for different protonated and deuterated $BP_{1-x}BPI_x$ crystals.

x	$\ln(\tau_0, \mathrm{s})$	T_0(K)	E_{b0}/k_B(K)	σ_{E_b}/k_B(K)
		Protonated compounds		
0.85	−25.91	5	490.99	32.57
0.7	−21.9	3.8	205.33	28.99
0.6	−22.44	2.6	187.55	26.58
0.5	−24.99	1.7	228.29	31.59
		Deuterated compounds		
0.85	−20.72	20.56	390.48	55.43
0.75	−23.06	8.15	425.27	72.68
0.7	−24.24	9.6	568	57
0.6	−23.7	9.8	459	49.6
0.5	−22.16	12.2	360.12	84.32

The temperature dependences of the average local potential asymmetry A_0 and the standard deviation σ_A are shown in Figs. 10–13.

The temperature dependence of the widths σ_A of the random asymmetry distribution of the local potentials is rather weak in the temperature range under study. However, in contradiction to usual proton glasses the average asymmetry A_0 of the local potentials of the hydrogen bonds is nonzero and remarkably temperature dependent. At the upper end of the studied temperature region, the average asymmetry A_0 is clearly larger than the widths σ_A of the random asymmetry distribution. With lower temperatures, A_0 becomes smaller than σ_A, but A_0 does disappear only for very low temperatures. This behavior, which is quite surprising and has not yet been observed for other dipolar glasses, is discussed in the following section.

V. DISCUSSION AND CONCLUSIONS

Considering the dielectric studies of protonated and deuterated $BP_{1-x}BPI_x$ mixed crystals published until now in the

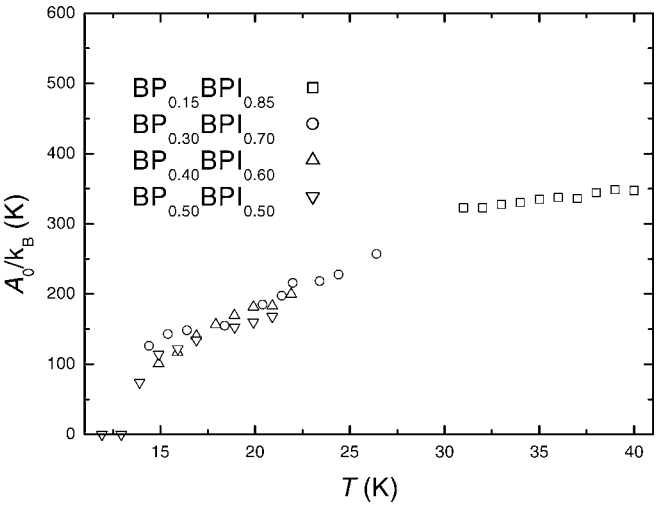

FIG. 10. The temperature dependencies of the average local potential asymmetry A_0 of protonated crystals.

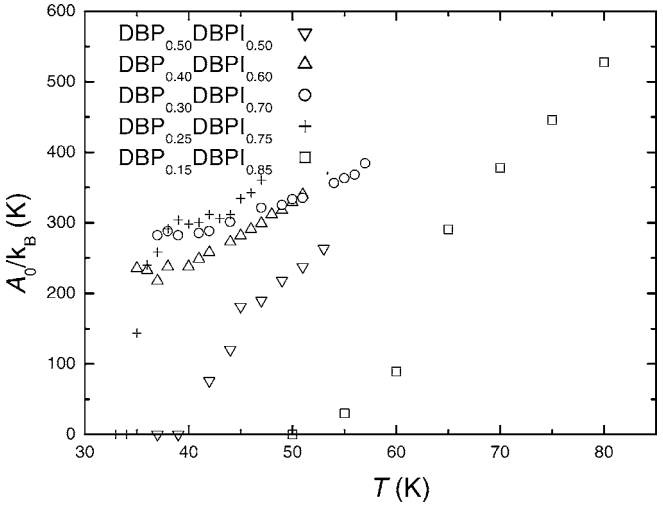

FIG. 11. The temperature dependencies of the average local potential asymmetry A_0 of deuterated crystals.

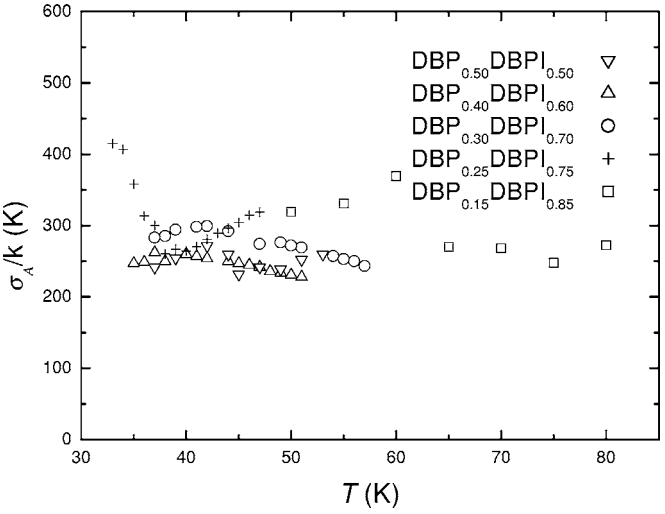

FIG. 13. The temperature dependencies of the standard deviation σ_A of deuterated crystals.

literature, at first glance these solid solutions seem to be typical representatives of the family of proton and deuteron glasses. In the middle region of composition, $0.9>x>0.3$, no anomaly in ε' indicating a polar phase transition can be detected down to the lowest temperatures. The freezing phenomena reveal the characteristics of a transition into a dipolar glass state. In the temperature region below 100 K, dispersion effects dominate the dielectric response in the frequency range below 1 MHz. The temperature behavior is typical for glasses. With decreasing measurement frequency, the maximum of ε' shifts to lower temperatures followed by the maximum of ε''. At fixed temperatures, the frequency dependence of ε' and ε'' provides clear evidence that the frequency dependence of ε'' is much broader then for Debye dispersion where the broadening increases considerably towards lower temperatures. The most probable dielectric relaxation time τ follows a Vogel-Fulcher law with Vogel-Fulcher temperatures that are considerably higher for the deuterated crystals in comparison to that one of the protonated crystals.

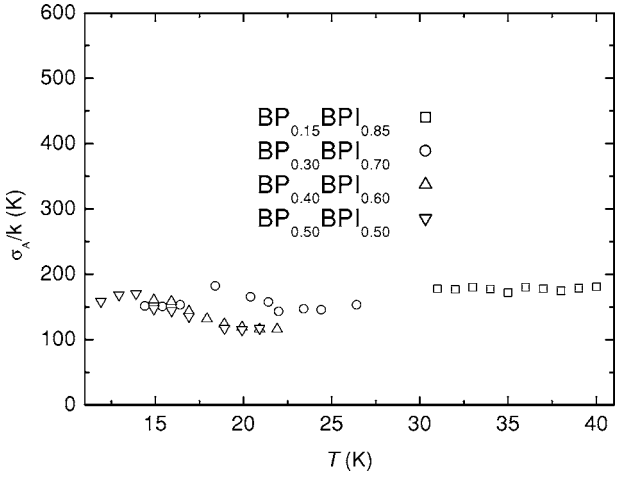

FIG. 12. The temperature dependencies of the standard deviation σ_A of protonated crystals.

But looking a bit more in detail, striking differences to the other proton glasses, e.g., of the KDP family, become apparent. The authors of Ref. 20 tried to interpret the temperature dependence of the static dielectric susceptibility within the framework of the RBRF Ising model. They found that rather large random fields play an important role. But even more unusual, for reasonable fits they had to consider a rather large long-range order contribution J_0 that is comparable to J. On the other hand, there are no characteristic differences of the quality of fits with the three- and one-dimensional RBRF models.

On the other hand, not only for the ferroelectric and antiferroelectric compositions but also for the compositions with glasslike behavior, they got reasonable fits of the static susceptibility using the quasi-one-dimensional Ising model of one-dimensional dipole chains with intrachain ferroelectric couplings stronger than interchain ones. The authors did not consider this interpretation any further because predictions resulted for antiferroelectric transitions at temperatures above 106 K where in fact no sign of a transition is present in ε' experiments.

Our present results show that the situation in the $BP_{1-x}BPI_x$ mixed crystals is even more peculiar. For all compositions under study, the fits deliver an average asymmetry A_0 of the local potentials that is almost linearly temperature dependent with about the same slope. Extrapolating the A_0 behavior of the protonated crystals to higher temperatures, the average interaction J_0 given by Eq. (12) meets with $\bar{p}=1$ about the values $J_0/k_B=200$ K and 212 K determined for $BP_{0.15}BPI_{0.85}$ and $BP_{0.40}BPI_{0.60}$, respectively, within the framework of the RBRF Ising model from ENDOR measurements. Obviously, these numbers are close to the intrachain coupling parameter $J_\parallel$ in BP and BPI. At the same time, the random bond interactions of both the crystals, $J/k_B=30$ K and 25 K, are much smaller than the random fields represented by $\sqrt{\Delta}/k_B=79$ K and 103 K, respectively, and both considerably smaller than the average ordering interaction J_0. Consequently, $BP_{0.15}BPI_{0.85}$ and $BP_{0.40}BPI_{0.60}$ do not behave like a true proton glass but undergo a transition into a phase

with coexisting long-range and glassy order. However, there is no anomaly of the dielectric permittivity detectable at the corresponding transition temperatures.

For the other mixed crystals under study, the situation is similar. Above about 20 K and 60 K for the protonated and deuterated mixtures, respectively, the mean asymmetry A_0 of the local potential of the O-H···O bonds is larger than the disorder term $\sigma_A = 2J\sqrt{q_E + \tilde{\Delta}}$, i.e., long-ranged order and glassy order do coexist below a temperature T_C that is close to J_0/k_B. For the protonated crystals, the transition temperatures from the paraelectric phase into the phase with coexisting long-range and glassy order were measured by ENDOR and spin-lattice relaxation measurements.[30] They range from 160 K for $BP_{0.15}BPI_{0.85}$ to 110 K for $BP_{0.70}BPI_{0.30}$.

However, if one remembers the chainlike structure of the compound and the quasi-one-dimensional behavior of the temperature dependence of the susceptibility in ferroelectric betaine phosphite and antiferroelectric betaine phosphate characterized by a strong ferroelectric intrachain coupling $J_\parallel$ but weak ferroelectric and antiferroelectric couplings $J_\perp \approx \pm J_\parallel/10$ between chains, the above explanation seems to be too simple. As the estimated random bond interaction J is of the same order of magnitude as the interchain coupling $J_\perp$, one can suspect a more complex order between chains, as, e.g., antiparallel or modulated alignment. Unfortunately, local information like the asymmetry of the local potential concluded from relaxation time distribution or the local polarization obtained by magnetic resonance experiments do not allow any conclusion to the relative polarization directions of the chains. Therefore, parallel and antiparallel arrangements of chains are undistinguishable with these investigations. Consequently, the experimental results presented above allow only the conclusion about a certain ferroelectric order of the hydrogen bonds within the chains but nothing about the order between the chains, i.e., a ferroelectric chain arrangement cannot be distinguished from an antiferroelectric or commensurately modulated one.

On the other hand, even if one is ignoring the coupling between chains and is considering them to be independent, at low temperatures some kind of order within the chains is expected in the form of rather large domains. Within the framework of the one-dimensional random-field Ising model,[43,44] the system is disordered at $T=0$ K but contains domains with a typical size given by the Imry-Ma length

$$L_{\mathrm{IM}} \approx \frac{4J_0^2}{\Delta}. \tag{15}$$

With $J_0/k_B \approx 220$ K and $\Delta \approx 3600$ K^2 the domain length within the chain results in $L_{\mathrm{IM}} \approx 50$ spin distances. With a local measurement one then sees ordered spins when the domain lifetime is longer than the time window of about 10^{-7} s for ENDOR measurements and 10^{-2}–10^{-7} s for dielectric spectroscopy, respectively.

As these domains are stabilized by the random fields caused by substituted phosphite groups in phosphate chains or vice versa, one may suspect that the appropriate couplings between neighboring chains also become stabilized leading to three-dimensional domains already at finite temperatures. As mentioned above, the transition from the paraelectric phase into this phase with a coexisting long-range and glassy order is related to an anomaly of the phonon system,[29–32] which give strong evidence for a cooperative transition. At the same time, the temperature dependence of the static susceptibility announces a kind of antiferroelectric transition at these temperatures. These together with all the other facts discussed above lead to the conclusion that for the whole composition range of $BP_{1-x}BPI_x$ below about 100 K a long-range ordered phase with a considerable degree of disorder does exist. This phase is characterized by a ferroelectric order of the bridging protons or deuterons within the phosphate/phosphite chains but with a nonferroelectric arrangement of neighboring chains.

The behavior towards very low temperatures provides a surprise. As Figs. 10 and 11 show, the average asymmetry A_0 and herewith the ferroelectric interaction J_0 within the chains decreases to lower temperatures. At 17 K and 40 K, for all the compositions of protonated and deuterated $BP_{1-x}BPI_x$, respectively, A_0 did cross σ_A, and became even smaller at lower temperatures. That means, the crystals are now in a phase with dominating glassy order. For certain compositions, A_0 goes to zero in the temperature range under study.

At first glance, it seems quite unusual that the degree of order is reduced at lower temperatures and finally a glassy state evolves at very low temperatures. Therefore, we must consider first that the result of our dielectric measurement is not an artifact of the measuring method. The methods used in this work to determine the effective distribution parameters of the H bonds are based on the measurements of the dynamic response of the protons or deuterons in the distorted double-well potential. From the experimental complex dielectric spectrum $\varepsilon^*(\nu)$ the relaxation-time distribution function $w(\tau)$ is calculated using the Tikhonov regularization technique. Due to intrachain ordering the majority of H bonds are asymmetric and give the main contribution to the proton dynamics at intermediate temperatures. Now at the lowest temperatures, when the asymmetry further increases, one could suspect that those protons or deuterons with the strongest asymmetry of the potential tend to freeze in the deep lower-energy minimum of the asymmetric H bonds. They are effectively excluded from the dielectric dynamics and do not contribute anymore to the $w(\tau)$ distribution function resulting in a seemingly reduced average asymmetry A_0. However, we know from the ENDOR results that the long-range order parameter already has the value $\bar{p}=0.7$ at 90 K such that it can hardly show a remarkable increase between 30 K and 15 K where A_0, determined with dielectric spectroscopy, decreases drastically. Furthermore, dielectric spectroscopy gives a value $A_0/k_B = 350$ K for $BP_{0.15}BPI_{0.85}$ at 40 K which is considerably larger than $A_0/k_B = \bar{p} \times 2J_0 = 0.7 \times 400$ K $= 280$ K determined with ENDOR spectroscopy at 90 K. The corresponding long-range order parameter value is $\bar{p} = 350/400 = 0.88$ at 40 K. Thus we can ascertain that dielectric spectroscopy gives correct parameters A_0 at low temperatures. Similar experimental results of another group of an at least partial erosion of the antiferroelectric order and a transition into a glassy state in a related mixed crystal $(\text{betaine arsenate})_{0.73}(\text{betaine phosphate})_{0.27}$ at low temperatures can be considered as further confirmation of our observation.[45]

For the sake of clarity one must finally note that the "local" measurements performed in the present paper and in the former ENDOR papers do not give information about the entire order parameter but only about the sublattice order parameter within the chains. Consequently, the analysis of the sublattice order parameter behavior within the framework of the three-dimensional RBRF Ising model is a contradiction in terms. The resulting model parameters J, J_0, and Δ have to be considered as very questionable, or at the utmost, as a projection of the three-dimensional RBRF order parameter behavior on the chain sublattice order behavior. Keeping this in mind, the diminishing ferroelectric long-range interaction J_0 can be interpreted in the following manner. A finite sublattice polarization of the chains is only possible for a three-dimensional system. At temperatures only slightly lower than J_0/k_B the interchain couplings are strong enough to enforce a three-dimensional order behavior. With lower temperatures the disordering forces between chains must become more and more important, leading to a reduced ferroelectric chain sublattice polarization. Finally, the three-dimensional long-range order breaks down with the result that no chain sublattice polarization can exist anymore at finite temperatures. One can suspect that the disappearance of chain sublattice polarization marks the transition into the nonergodic glassy state.

The present theoretical models are not able to give a satisfactory description of these phenomena in our proton and deuteron glasses. However, one can hazard a guess that the observed transition from an inhomogeneous long-range ordered ferric state to a glassy state at very low temperatures bears a certain resemblance to the long puzzling question of the self-generated disorder and glassiness in structural glasses.[46–49]

ACKNOWLEDGMENT

This work was supported by the Alexander von Humbold Stiftung.

*Electronic address: juras.banys@ff.vu.lt

[1] J. Albers, A. Klöpperpieper, H. J. Rother, and K. Ehses, Phys. Status Solidi A **74**, 533 (1982).
[2] J. Albers, A. Klöpperpieper, H. E. Müser, and H. J. Rother, Ferroelectrics **54**, 45 (1984).
[3] J. Albers, A. Klöpperpieper, H. J. Rother, and S. Haussühl, Ferroelectrics **81**, 27 (1988).
[4] D. Schaack, Ferroelectrics **104**, 147 (1990).
[5] S. L. Hutton, I. Fehst, R. Böhmer, M. Braune, B. Mertz, P. Lunkenheimer, and A. Loidl, Phys. Rev. Lett. **66**, 1990 (1991).
[6] M. L. Santos, J. C. Azevedo, A. Almeida, M. R. Chaves, A. R. Pires, H. E. Müser, and A. Klöpperpieper, Ferroelectrics **108**, 1969 (1990).
[7] M. L. Santos, M. R. Chaves, A. Almeida, A. Klöpperpieper, H. E. Müser, and J. Albers, Ferroelectr., Lett. Sect. **15**, 17 (1993).
[8] A. Loidl and R. Böhmer, in *Disorder Effects on Relaxational Processes*, edited by R. Richert and A. Blumen (Springer, Berlin, 1994), p. 659.
[9] H. Ries, R. Böhmer, I. Fehst, and A. Loidl, Z. Phys. B: Condens. Matter **99**, 401 (1996).
[10] W. Schildkamp and J. Spilker, Z. Kristallogr. **168**, 159 (1984).
[11] I. Fehst, M. Paasch, S. L. Hutton, M. Braune, R. Böhmer, A. Loidl, M. Dörffel, Th. Narz, S. Haussühl, and G. J. McIntyre, Ferroelectrics **138**, 1 (1993).
[12] M. Lopes dos Santos, J. M. Kiat, A. Almeida, M. R. Chaves, A. Klöpperpieper, and J. Albers, Phys. Status Solidi B **189**, 371 (1995).
[13] G. Fischer, H. J. Brückner, A. Klöpperpieper, H. G. Unruh, and A. Levstik, Z. Phys. B: Condens. Matter **79**, 391 (1990).
[14] H. Bauch, J. Banys, R. Böttcher, A. Pöppl, G. Völkel, C. Klimm, and A. Klöpperpieper, Ferroelectrics **163**, 59 (1995).
[15] K. Binder and J. D. Reger, Adv. Phys. **41**, 547 (1992).
[16] R. Blinc, Z. Naturforsch., A: Phys. Sci. **45a**, 313 (1989).
[17] R. Pirc, B. Tadic, R. Blinc, and R. Kind, Phys. Rev. B **43**, 2501 (1991).
[18] R. Blinc, R. Pirc, B. Tadic, B. Zalar, D. Arčon, and J. Dolinšek, Crystallogr. Rep. **44**, 177 (1999).
[19] M. Oreŝič and R. Pirc, Phys. Rev. B **47**, 2655 (1993).
[20] J. M. B. Lopes dos Santos, M. L. Santos, M. R. Chaves, A. Almeida, and A. Klöpperpieper, Phys. Rev. B **61**, 8053 (2000).
[21] J. Banys, C. Klimm, G. Völkel, H. Bauch, and A. Klöpperpieper, Phys. Rev. B **50**, R16751 (1994).
[22] A. V. de Carvalho and S. R. Salinas, J. Phys. Soc. Jpn. **44**, 238 (1978).
[23] R. Blinc, B. Žekš, A. Levstik, C. Filipič, J. Slak, M. Burgar, I. Zupančič, L. A. Shuvalov, and A. I. Baranov, Phys. Rev. Lett. **43**, 231 (1979).
[24] R. Blinc and F. C. Sa Baretto, J. Chem. Phys. **72**, 6031 (1980).
[25] D. Sherrington and S. Kirkpatrick, Phys. Rev. Lett. **35**, 1792 (1975).
[26] H. Bauch, G. Völkel, R. Böttcher, A. Pöppl, H. Schäfer, J. Banys, and A. Klöpperpieper, Phys. Rev. B **54**, 9162 (1996).
[27] G. Völkel, H. Bauch, R. Böttcher, A. Pöppl, H. Schäfer, and A. Klöpperpieper, Phys. Rev. B **55**, 12151 (1997).
[28] G. Völkel, N. Alsabbagh, J. Banys, H. Bauch, R. Böttcher, M. Gutjahr, D. Michel, and A. Pöppl, in *Adv. in Solid State Phys. 42*, edited by B. Kramer (Springer-Verlag, Berlin, 2002), pp. 241–251.
[29] A. Pöppl, G. Völkel, J. Hoentsch, S. Orlinski, and A. Klöpperpieper, Chem. Phys. Lett. **224**, 233 (1994).
[30] J. Banys, A. Pöppl, G. Völkel, J. Simon, J. Hoentsch, and A. Klöpperpieper, Lith. Phys. J. **36**, 409 (1996).
[31] R. Böttcher, A. Pöppl, G. Völkel, J. Banys, and A. Klöpperpieper, Ferroelectrics **208**, 105 (1998).
[32] J. Banys, S. Kamba, A. Klöpperpieper, and G. Völkel, Phys. Status Solidi B **231**, 581 (2002).
[33] J. Banys, S. Lapinskas, A. Kajokas, A. Matulis, C. Klimm, G. Völkel, and A. Klöpperpieper, Phys. Rev. B **66**, 144113 (2002).
[34] H. Schäfer, E. Sternin, R. Stannarius, M. Arndt, and F. Kremer, Phys. Rev. Lett. **76**, 2177 (1996).
[35] B. G. Kim, J. J. Kim, D. H. Kim, and H. M. Jang, Ferroelectrics **240**, 249 (2000).

[36] R. Pelster, T. Kruse, H. G. Krauthaeuser, G. Nimtz, and P. Pissis, Phys. Rev. B **57**, 8763 (1998).
[37] A. V. Tichonov, Dokl. Akad. Nauk SSSR **153**, N3 (1963).
[38] C. L. Lawson and R. J. Hanson, *Solving Least Squares Problems* (SIAM, Philadelphia, 1995).
[39] S. W. Provencher, Comput. Phys. Commun. **27**, 213 (1982).
[40] Z. Kutnjak, R. Pirc, A. Levstik, I. Levstik, C. Filipič, R. Blinc, and R. Kind, Phys. Rev. B **50**, 12421 (1994).
[41] R. Kind, P. M. Cereghetti, C. A. Jeitziner, B. Zalar, J. Dolinsek, and R. Blinc, Phys. Rev. Lett. **88**, 195501 (2002).
[42] J. Dolinšek, D. Arčon, B. Zalar, R. Pirc, R. Blinc, and R. Kind, Phys. Rev. B **54**, R6811 (1996).
[43] T. Nattermann, in *Spin Glasses and Random Fields*, edited by A. P. Young (World Scientific, Singapore, 1998), Vol. 12.
[44] D. S. Fisher, P. Le Doussal, and C. Monthus, Phys. Rev. E **64**, 066107 (2001).
[45] M. Manger, S. Lanceros-Mendez, G. Schaack, and A. Klöpperpieper, J. Phys.: Condens. Matter **8**, 4617 (1996).
[46] A. A. Pastor, V. Dobrosavljevic, and M. L. Horbach, Phys. Rev. B **66**, 014413 (2002).
[47] V. G. Rostiashvili, G. Migliorini, and T. A. Vilgis, Phys. Rev. E **64**, 051112 (2001).
[48] M. Tarzia and A. Coniglio, cond-mat/0506485 (unpublished).
[49] V. G. Rostiashvili and T. A. Vilgis, cond-mat/9911280 (unpublished).